Smart Structures and Systems, *Vol. 13, No. 6 (2014) 1041-1063*
DOI: http://dx.doi.org/10.12989/sss.2014.13.6.1041

Two-module robotic pipe inspection system with EMATs

Jin-Hyuk Lee[1], Sangchul Han[2],
Jaekyu Ahn[2], Dae-Hyun Kim[3**] and Hyungpil Moon[*2]

[1]*Graduate School of Energy and Environment, Seoul National University of Science and Technology 232 Gongneung-ro, Nowon-gu, Seoul 139-743,Republic of Korea*
[2]*School of Mechanical Engineering, Sungkyunkwan University, Seoburo 2066, Jangan-gu, Suwon 440-746, Republic of Korea*
[3]*Department of Mechanical and Automotive Engineering, Seoul National University of Science and Technology, 232 Gongneung-ro, Nowon-gu, Seoul, 139-743, Republic of Korea*

(Received December 13, 2013, Revised March 15, 2014, Accepted April 30, 2014)

Abstract. This work introduces a two-module robotic pipe inspection system with ultrasonic NDE device to evaluate the integrity of pipe structures. The proposed robotic platform has high mobility. The two module mobile robot platform overcomes pipe obstacle structures such as elbow, or T-branch joints by cooperative maneuvers. Also, it can climb up the straight pipeline at a fast speed due to the wheel driven mechanism. For inspection of pipe structure, SH-waves generated by EMAT are applied with additional signal processing methods. A wavelet transform is implemented to extract a meaningful and specific signal from the superposed SH-wave signals. Intensity ratio which is normalized the defect signals intensity by the maximum intensity of directly transmitted signals in the wavelet transforms spectrum is applied to evaluate defects quantitatively. It is experimentally verified that the robotic ultrasonic inspection system with EMAT is capable of non-destructive inspection and evaluation of defects in pipe structure successfully by applying signal processing method based on wavelet transform.

Keywords: out- pipe robot; EMAT; wavelet transform; two-module climbing robot; non-eestructive test robotic system

1. Introduction

Large scale plants including power plants are made up of many pipes. Non-destructive tests using ultrasonic waves have been implemented to inspect the integrity of pipe structures. However, conventional ultrasonic inspections have been implemented by manual work usually, so it is hard to be done in high temperature or dangerous areas. Furthermore, ultrasonic testing would not be possible during facilities in-service operating. To avoid these disadvantages, it would be beneficial to develop an automated ultrasonic inspection system that uses robots. A robotic pipe inspection system requires two main functions; the mobility of the robot needs to be good enough to cover

*Corresponding author, Professor, E-mail: hyungpil@me.skku.ac.kr
** Co-corresponding author, Professor, E-mail: dkim@seoultech.ac.kr

Copyright © 2014 Techno-Press, Ltd.
http://www.techno-press.org/?journal=sss&subpage=8 ISSN: 1738-1584 (Print), 1738-1991 (Online)

the extensive regions of the pipe structures and the non-destructive test equipment needs to be compatible with robotic mobile platforms.

There have been developed two major types of pipe inspections robots (Kim and Choi 2005, Roh *et al.* 2009); one is the in-pipe robot which maneuvers inside of the pipelines and the other is the out-pipe robot which is attached to the outside of the pipe surface and maneuvers on the pipelines. The major advantage of in-pipe robots is that they do not need special mechanisms to overcome the pipe installation structures such as hangers, flanges, and valves (Roh and Choi 2005). However, in-pipe robots require special equipment or structures to be deployed into the pipelines and they are functional in often cases while the pipeline services stop or even after the pipelines are emptied (Parker and Graper 1998). Out-pipe robots can perform inspections while the pipelines are in operation and they do not require special equipment for deployment. However, they need to be able to overcome obstacles on the pipeline out-surface as well as move from one pipeline to another over T-branch or elbow joint pipes which are not so trivial tasks as for in-pipe robots.

Many types of out-pipe climbing robots have been developed. A four-wheel based climbing robot is developed (Xu and Wang 2008). The wheel units and the body structure of the robot enclose the pipeline in this robot. A six-wheel three-limb enclosed type pipe climbing robot (Noohi *et al.* 2010) and a four-wheel four-limb enclosed type pipe climbing robot (Kawasaki and Murakami 2008) have been introduced. Such closed-formation robots may move stably on the pipeline, but it is almost impossible to move from one branch of the pipelines to another, for example, over a T-branch without breaking such enclosure structures. Many robots with bio-inspired mechanisms have been also developed. A snake robot (Lipkin *et al.* 2007) forms a helical configuration and wraps around the pipe to roll along the pipe inside and outside. Although the climbing motion is relatively fast, no ultrasonic non-destructive evaluation (NDE) test has been demonstrated so far in such snake-like robots. A gecko robot (Kim *et al.* 2007) has a very interesting grasping and climbing mechanism, but its payload is not high enough for ultrasonic NDE tests. Robots having inch-worm like motion (Fukuda *et al.* 1987, Tavakoli *et al.*2011) are also popular, but their motion is slow.The maximum climbing speed of 3DCLIMBER is only 1m/min (Tavakoli *et al.* 2011).

Nondestructive test equipment for robotic inspection should be also carefully selected to facilitate automated inspection. Conventional ultrasonic probes such as angle beam ultrasonic testing transducers require couplants for impedance matching between the transducer and the testing material as well as extended range of scanning motions over the surface of the testing material. Such conditions require the water-proof design of the robotic platform and also a high degree of freedom complicated manipulator for probe placing. On the other hand, an electromagnetic acoustic transducer (EMAT) generates ultrasonic waves without couplants. It can also generate various types of ultrasonic modes according to the shape and configuration of magnets and coils. The shear horizontal wave (SH-wave) could be generated by EMAT which can be transferred as a type of plate wave in thin sheet materials(Hirao and Ogi 2003, Hirao and Ogi 1999, Fujikawa 2002). Therefore, it is possible to perform tests over an entire range of thickness without switching several transducers back and forth. It means that SH-waves can make an automated inspection system move and control easier. However, the SH-wave signals are hard to evaluate the position or the size of defects simply, because the signals may include a superposition of various modes. Also, the modes can vary due to changes of frequency and velocity in response to variations in the thickness of the material (Hirao and Ogi 2003, Hirao and Ogi 1999, Fujikawa 2002, Lee *et al.* 2011, Park *et al.* 2006). Therefore, lots of researchers have used several signal-processing methods to analyze EMAT signals and extract the key features from complicated defect-signals (Lei *et al.* 2008, Soto-Cajiga *et al.* 2012,Liu *et al.* 2013). However, it is still difficult to evaluate defects quantitatively.

In this paper, we introduce a two-module robotic pipe inspection system (see Fig. 21) with EMAT sensors which is used for inspecting pipelines where human workers cannot perform manual inspection easily. The robotic platform of our system is composed of two-module with a joining linkage mechanism and attached to the outer surface of pipelines to move over flanges, T-branch joints, and elbow joints. Each module has two types of arm-structures, 'climbing arm' and 'rotation arm', and they are used for attaching the robotic system on the surface of the pipe (see Fig. 22). Wheels are employed in each arm-structure and the two-module robot can move fast on the straight pipe lines. Unlike other fast moving wheel-based out-pipe robots, our system is configured in an open-formation, *i.e.* the robot does not enclose the pipeline.

The robotic system can perform non-destructive inspection of pipelines with EMAT sensors. A transducer that generates SH-EMAT signals is developed for the robotic application and the signals are evaluated. The magnetic coils of EMAT are embodied inside the robotic mobile platform when traveling and they protrude to be located above the surface of pipe when performing tests. While moving along the pipeline, the magnetic adhesion force between the EMAT sensor coil and the pipe surface tends to hinder the robot locomotion. Thus, the EMAT sensors are mechanically connected to the climbing arm and loose the contact with the pipe surface when the climbing arm is engaged with the pipe. The SH wave signals are successfully measured and evaluated for detecting defects in the pipelines.

This paper is composed of five sections. In section 2, we introduce the detail design of the out-pipe robot, its maneuverability, and strategy for overcoming obstacle joints of the pipelines. In section 3, signal processing methods are described to analyze the SH-wave signals. To evaluate complicated SH-wave signals due to the dispersion of modes and the duplication of signals, wavelet transform signal processing methods are applied and the intensity of the signal between the transmitter and the receiver is used. Experimental testing results using robotic inspection system is given in Section 4 and the contribution of our work is summarized in Section 5.Note that two different tests are conducted for EMAT sensor evaluation. One is for the sensor design presented in 3.2 and the other is to verify the performance of the sensor in the robotic inspection system and presented in 4.1.

2. Robotic system

2.1 Robot design

Pipelines in nuclear power plants or in chemical plants usually form complex pipe network structures consisting of straight pipe, flanges, valves, L-shape, and T-shape joints. Also, there are fixtures to hold the pipelines on the wall or floor. Pipe inspection systems must traverse over such complicated obstacles on the pipelines and be able to move from one branch of the pipelines to another. Therefore, the high mobility of the pipe inspection robot is one of the most critical functions that the system must have. Our design concept for high mobility is to combine the advantage of the fast wheel-based locomotion and the high maneuverability of the inch-worm type arm grasping. To move from one branch to another, the robot must have two degree of freedom of motion, circumferential and axial motion, and one of the two modules must be attached to the pipe at all times. The open-formation type design also increases the mobility of the robot because one of the modules can be detached from the pipeline and move over the obstacle structure of the pipeline. In this section, the detail of robot design is discussed.

A schematic figure of our robot design is illustrated in Fig. 1. Two moving mobile robot platforms are linked by a‘connecting arm’ as shown in Fig. 1(a). Each module is attached to the pipe by either ‘climbing arm’ or ‘rotation arm’ depending on the task. Two sets of ‘climbing arm’ is used for holding the robot when it moves along the pipeline as shown in Fig. 1(b). There are four wheels are attached to the one set of ‘climbing arm’ and one in each limb is actively driven by a DC motor. The climbing arms are driven by worm and worm gear mechanism. When the robot performs NDE test using EMAT sensors, one set of ‘rotation arm’ where four wheels reside in circumferential direction is used for holding the pipe and driven by a ball-screw and linear guide mechanism. In this case, climbing arms are detached from the pipe as shown in Fig. 1(c). Therefore, each moving module has two degree of freedom in motion; the direction along the pipe and the circumferential direction. The mechanisms used for climbing and rotation arms have high gear ratio with small backlash and provide suitable amount of force in grasping the pipe. The surface of the wheels are made of polyurethane to increase the friction between the wheel and the pipe. Also, the wheel-driven motion of our system is faster than that of inch-worm type of locomotion when moving along the straight pipeline. When the two-module robot moves from one branch to another at a T-branch joint, one module holds and rolls on the pipe, then the ‘connecting arm’ lifts up the other module. When the other module reaches the pipe, two module switches holding of the pipes as shown in Fig 1(d). The ‘connecting arm’ is composed of a four-bar linkage mechanism which is designed to maximize the mechanical advantage through the whole lifting-up process. Each module of the mobile robot platform maintains strong holding force to the pipe so that it can move along the pipeline with lifting up the other module at all configurations. Elbow joints are also overcome in a similar fashion.

The configuration of our robot is asymmetric about the axis of the pipeline and open-formation unlike other closed-formation pipe climbing robots. The mass center of the robot lies off the center of the pipeline axis. When the holding force from the ‘climbing arm’ or ‘rotation arm’ is not controlled properly, the pose of the robot becomes inclined from the pipeline and is easy to fall off from the pipe as shown in Fig. 2(b). To hold the robot parallel to the axis of the pipeline as shown in Fig. 2(a) and to safely climb and move along the pipe, the robot needs to control the grasping force evenly distributed among the wheels. Stain gauge-based force sensors are installed on each limb of ‘climbing arm.’ Although our robot has only one degree of freedom in grasping the pipeline, simply open and close, it can grasp the pipe stably by alternatively using two grasping mechanisms – by climbing arm and by rotation arm, when needed. Fig. 2(a) shows the case of stable grasping and Fig. 2(b) shows the case of unstable climbing pose. In case of Fig. 2(b), the robot falls off from the pipe when driving further upward. We control the robot’s grasping posture by measuring and controlling the grasping force on each ‘climbing arm.’ In each module, two sets of ‘climbing arms’ exist and strain gauges are attached on each arm to form half bridge circuits. Each climbing arms is controlled in its position, but the strain gauges generate signals proportional to its deformation which can be a measure of grasping force. Instead of developing an accurate force calibration model as a conventional force sensors, we experimentally find a stable level of the strain gauge signal when the robot stably climbs along the vertical pipeline.

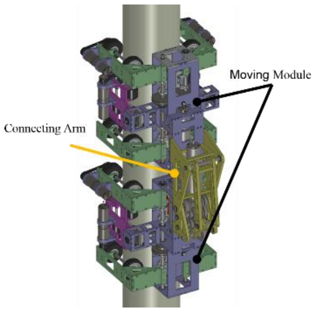

(a) Two-module inspection robot

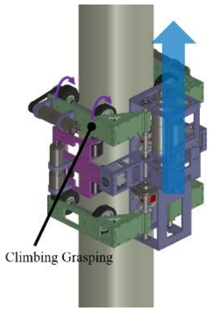

(b) Moving module climbing along the pipe

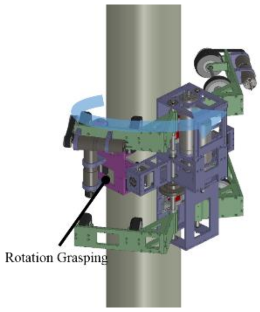

(c) Moving module rotating around the pole

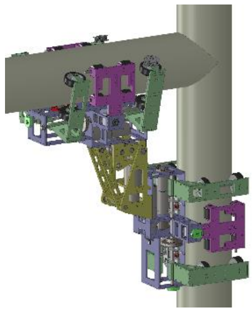

(d) Moving from one branch to another at a T-branch

Fig. 1 Two-Module inspection Robot: CAD model

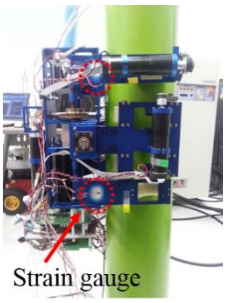

(a) Stable climbing

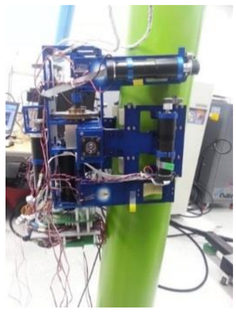

(b) Unstable climbing

Fig. 2 Stable and unstable climbing pose

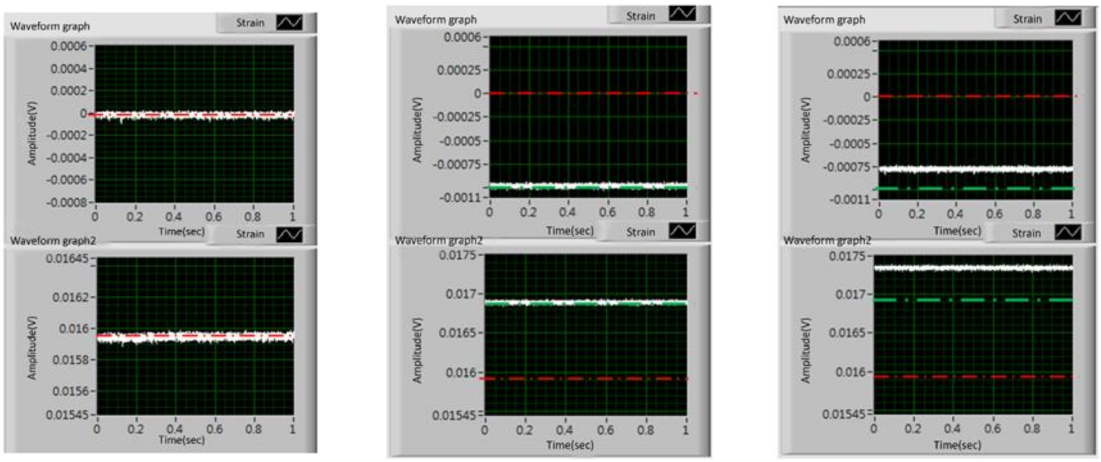

(a) Before grasping (b) Stable grasping (c) Unstable grasping

Fig. 3 Strain gauge signals when grasping the pipe; red dashed lines represent the zero-force level, green dash-dot lines represent the level of stable grasping, and the white lines represent the measurement signal. The labels in x-axis are all time (sec) and those of the y-axis are all the amplitude of the strain gauge signal (V).

In Fig. 3, raw signals of strain gauges are shown when the 'climbing arm' is not engaged with the pipe (non-grasping situation, Fig. 3(a)), when the climbing arm is stably grasping the pipe (Fig. 3(b)), and when the climbing arm is unstably grasping the pipe (Fig. 3(c)). In the unstable grasping case, the upper leg begins losing the grasping force as the wheel is slipping away from the pipe and, at the same time, an exceeding grasping force (larger than the necessary grasping force that corresponds to the green dash-dot line in Fig. 3) is exerted to the low leg. When the climbing arm of the robot unstably grasps the pipe, its pose becomes the one in Fig. 2(b) and the strain gauge signals of the climbing arm become the ones in Fig. 3(c). Because the climbing leg deforms in the elastic deformation region when grasping, the strain gauge signals reliably provide the grasping status. Using this strain gauge signals, we could succeed in making the robot stably moving along the vertical, horizontal, and inclined pipelines.

2.2 EMAT sensor installment in robot module

Three main issues must be resolved for robotic NDE testing with EMAT sensors. First, the EMAT transducers should maintain a constant distance to the pipe surface as well as between the transmitter and the receiver. Second, EMAT transducers should cover all the testing surface of pipe which requires axial directional motions and circumferential directional motions of the sensors. Third, the strong magnetic force of EMAT transduces must be considered in EMAT sensor installation because it may disturb the robot's locomotion. To resolve these issues, we design the EMAT installment for our mobile robot platform. The distance between the transmitter and the receiver transducers are fixed as the transmitter is installed in one robot module and the receiver is installed in the other. In order to maintain the contact distance between the transducers and the pipe surface, each EMAT sensor installment is linked to the climbing arm linkage system as depicted in Fig. 4(a). As the NDE test is performed circumferentially, the contact distance between the EMAT sensor and the pipe surface should be maintained while the robot is rotating about the pipe axis. In this case, the 'climbing arm' is disengaged with the pipe. Therefore, the position of the EMAT sensor installment can be controlled independently from the rotational motion of the robot (Fig. 4(c)). The contact force between the sensor and the pipe surfaces is maintained by a spring. As the climbing arm is controlled based on its position, it is reasonable that the compliant element is used for maintaining the contact force. Moreover, when the robot modules climb or move along the pipe, the climbing arm is engaged with the pipe and the EMAT sensor installment moves inside of the robot body (Fig. 4(b)). In this case, the strong magnetic force from the EMAT sensor does not disturb the robot's locomotion.

2.3 Robotic pipe inspection system locomotion test

The robot system is composed of two modules linked together by a connecting arm. The total robot weight including EMAT sensors is 30 kg and its size is $77 \times 38 \times 40$ cm. Each module has two actuators for climbing motion, two actuators for circumferential motion, and two actuators for generating grasping force. Including the one actuator for the connecting arm, total 13 actuators are used. All the actuators are DC motors and Maxon DC 150 W motors are used for the connecting arm, the climbing arms, and the rotation arms. Maxon DC 60 W motors are used for the remaining wheel driving actuators. The robot control unit is remotely interfaced with an external operating PC via CAN communication protocol. Controlling the robot in a wireless fashion is not currently implemented but can be done without difficulties in near future.

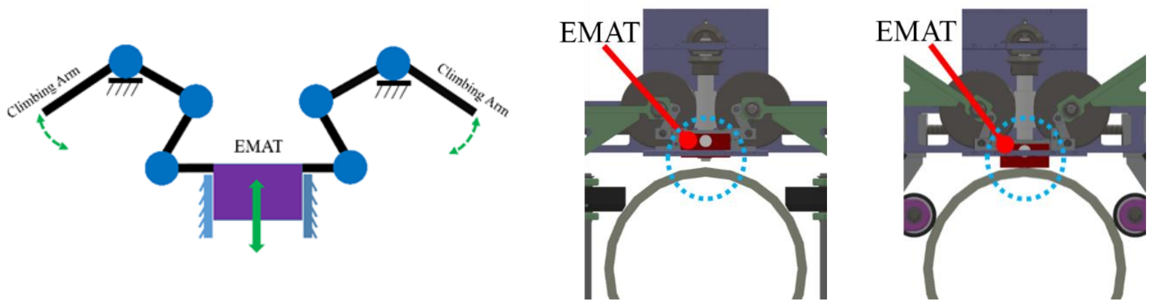

(a) EMAT Moving mechanism concept (b) Climbing (c) Rotation

Fig. 4 EMAT Moving mechanism

The sequence of inspection is as follows. The robot platform moves along the pipeline and places itself on a target inspection spot. In this process, the climbing arms are engaged with the pipe. The rotation arms switches to grasp the pipe and the climbing arm position is controlled so that the EMAT sensors are properly placed on top of the pipe surface. The robot finally performs the test while rotating circumferentially about the pipe. The sensing data obtained during this process are shown in Figs. 5 through 8. Fig. 5 shows the climbing arm position and the grasping measurement from the strain gauge sensor. Initially, the climbing arm is not engaged with the pipe and after moving about 32° the climbing arm is completely engaged with the pipe. It can be verified from the strain gauge signal which stably maintains about 2.9 V signal in the half-bridge circuit when the robot stably climbs up and down the pipe (Fig. 5). When the robot reaches the testing spot, it switches the holding mechanism to the rotation arm staring at time 58 sec (Fig. 7). In this process, the climbing arm is detached from the pipe and the stain gauge signal verifies the release of the holding force. At time 230 sec, the climbing arm begins detaching process. At this point, the strain gauge signal is high because the climbing arm is still in deformation. It loses contact force at about time 278 sec. The robot rotates about the pipe in circumferential direction and performs NDE tests (Fig. 8). After completing the test, the robot switches back to the climbing grasping and moves along the pipe. In Fig. 6, it is shown that the robot can move at speed of 12 cm/s.

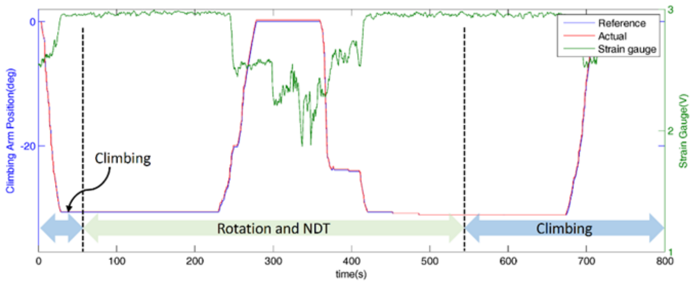

Fig. 5 Climbing arm position and the grasping measurement from the strain gauge sensor

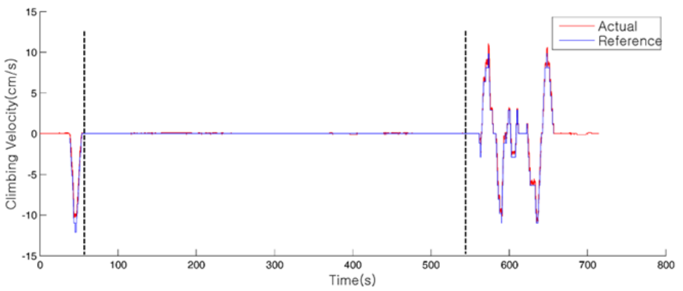

Fig. 6 Climbing velocity of the robot module

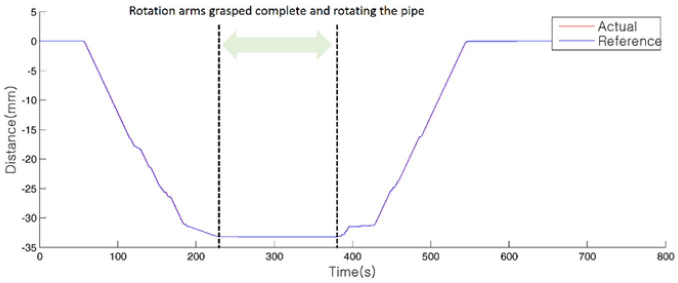

Fig. 7 Rotation arm position

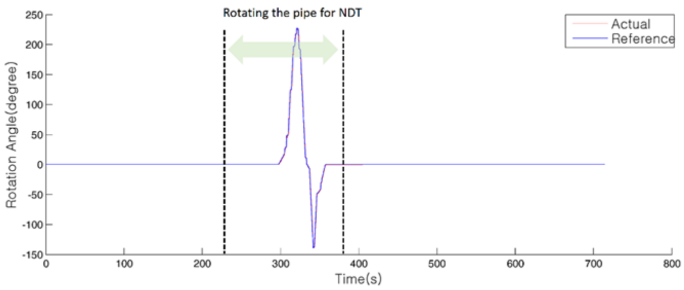

Fig. 8 Rotating angle of the robot module during the NDE test

3. NDE-EMAT System

3.1 EMAT design and setup

EMAT consists of two important elements, a coil and magnets. A shape of the coil determines a mode of ultrasonic wave. As alternating currents are generated in a coil by approaching an EMAT to a conductor, eddy currents are induced on the surface of the material, and a static magnetic field is applied to the eddy currents. Then the Lorentz force is also applied to the particles on the surface. When SH-waves are generated by using the Lorentz force in a plate, the force is perpendicular to the forwarding direction, and is transferred to a sample to be tested by turning the force 180° for every specific interval (a half-wavelength period). Thus, as illustrated in Fig. 9, an arrayed magnet that turns its polarity is required. The direction of the Lorentz force can be changed by the alternating current in a coil that is close to the surface of a structure; the alternating force plays a role of transmitting SH-waves as a source to generating ultrasonic waves. Also, the SH-wave could be transferred as a type of plate wave in thin sheet materials. It means that SH-waves can make an automated inspection system move and control easier.

As ultrasonic waves are induced in a region that is magnetized by the EMAT magnet, the magnetic field in a conductor can be described by the phase of the ultrasonic waves. Then, additional electric fields can be excited in the conductor. Using Maxwell’s equations, the magnetic field and the electric field in the conductor can be obtained. The equations satisfy the boundary condition for the conductor surface vibrated on the lower side and can be transformed to the electric and magnetic fields in the air where the EMAT coil is located. That is, the vibration of the ultrasonic wave is determined as electric and magnetic fields in the air and these are finally received by the EMAT coil. So, the EMAT can generate and receive ultrasonic waves without couplants (Hirao and Ogi 2003, Fujikawa 2002, Lee *et al.* 2011, Park *et al.* 2006).

In this study, a spiral coil is designed to generate Lorentz's force which makes SH-waves. In order to make high-precision coil, a printed-circuit technique is applied. The neodymium-iron-boron (Nd-Fe-B) magnets are applied to make a high power magnetic field. Fig. 10 shows the applied coil and magnets. Here, a thickness of magnet is designed according to a center-frequency of ultrasonic wave because the thickness of the magnet is related to a wavelength of the wave. Also, a case is designed to apply the magnets and coil as an EMAT. To consider of applying the sensor to the robot system, the size of the case is designed. Fig. 11 shows the design and a picture of the finally manufactured case.

In the robot system, two EMATs are set up at a fixed distance, as shown in Fig. 12. The transmitting EMAT generates SH-waves into the pipe wall and then the receiving EMAT acquires the SH-waves. The received SH-waves signals include both waves that are directly transmitted from the transmitting EMAT to the receiving EMAT, and waves reflected from a flaw. So, any defects can be detected by analyzing the signals of the reflected waves (Park *et al.* 2006, Gori *et al.* 1996).

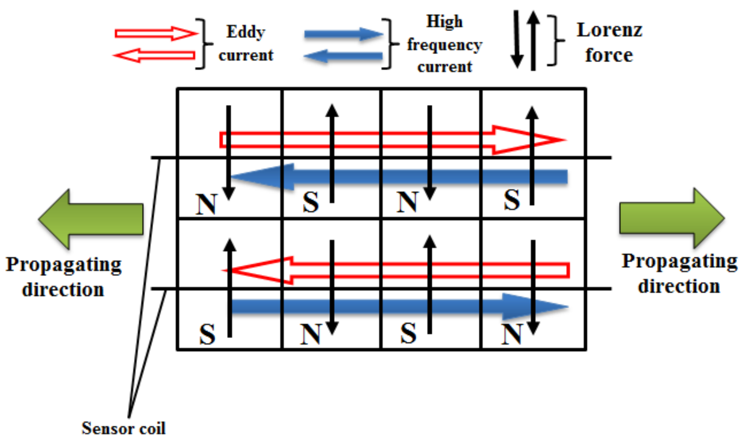

Fig. 9 Structure of the Lorenz type EMAT for generating SH waves

(a) magnets

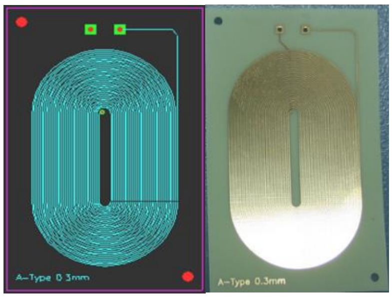

(b) coil

Fig. 10 Magnets and coil to construct EMAT

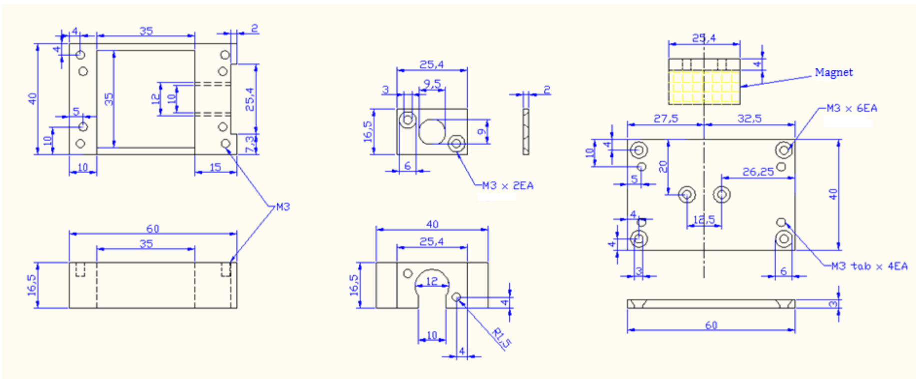

(a) Drawing of EMAT case

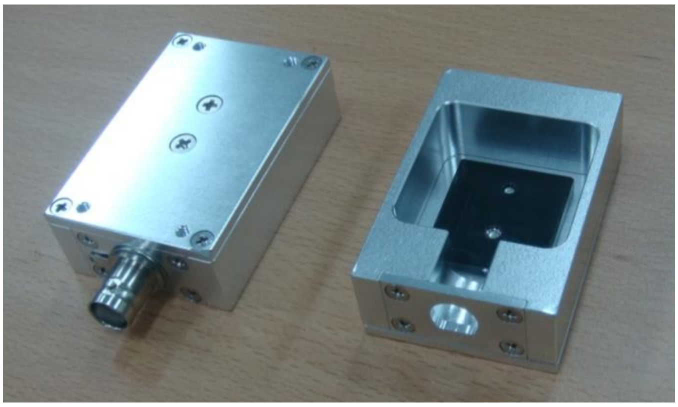

(b) Picture of EMAT case

Fig. 11 EMAT case

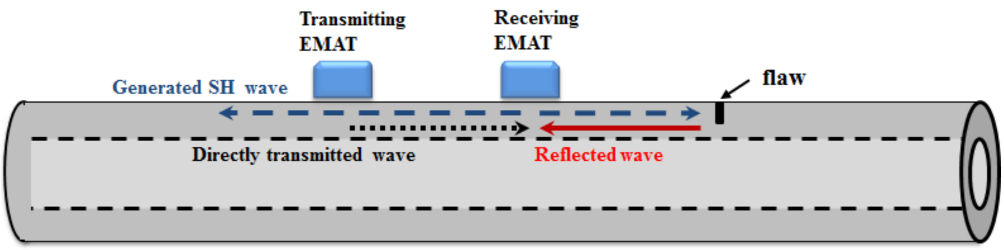

Fig. 12 EMATs setup for pipe inspection

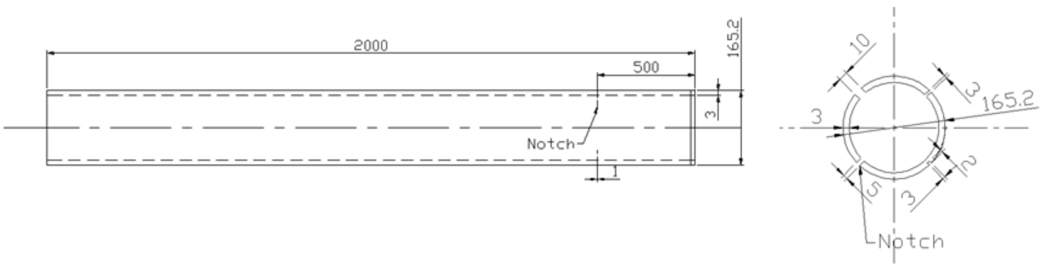

(a) Drawing flaws in pipe

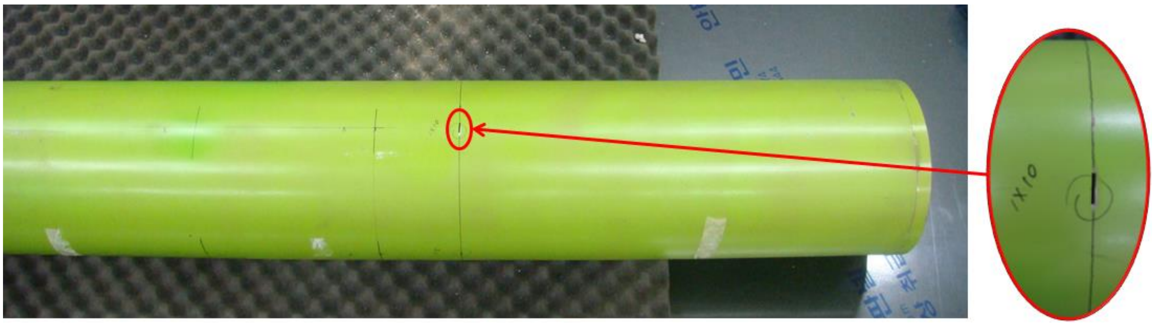

(b) Picture of pipe with flaws

Fig. 13 pipe specimen with flaws

3.2 Pipe Inspection using SH-EMAT

3.2.1 Specimen and test setup

A pipe-specimen with defects is manufactured for the SH-EMAT test by applying simulated defects. The specifications of the specimen, STS304 stainless steel pipe with 165.2 mm outer diameter and 3 mm thickness, are those used largely in plants.

The SH-waves generally work as a type of plate wave in thin sheets like a pipe. Therefore the intensity of the wave signal reflected from a defect depends on the vertical area of the defect versus the wave propagation direction. To consider a reflection from defects, the defects were manufactured as a type of notch in the pipe which having various areas including 3 mm × 2 mm (length of circumferential direction × depth), 3 mm × 3 mm, 5 mm ×3 mm and 10 mm ×35 mm, using electrical discharge machining (EDM). Fig. 13 shows the drawing of a pipe-specimen and the picture of the manufactured specimen with flaws.

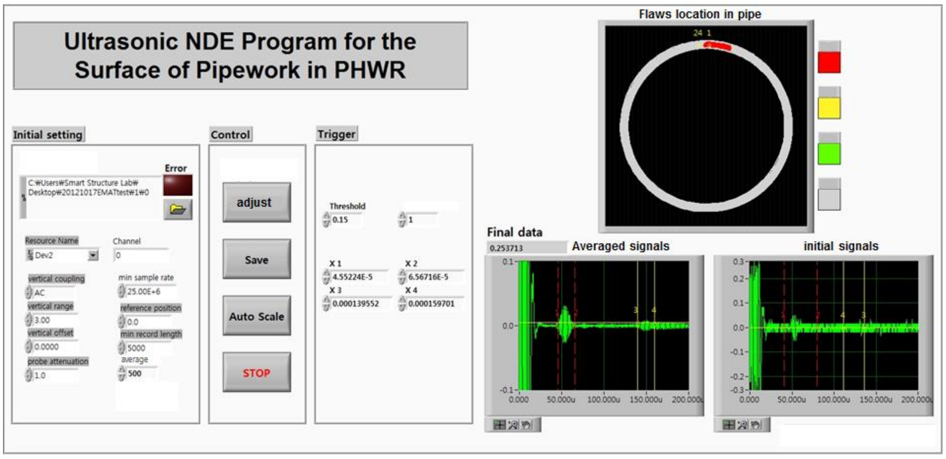

Fig. 14 Data Acquisition and signal processing software

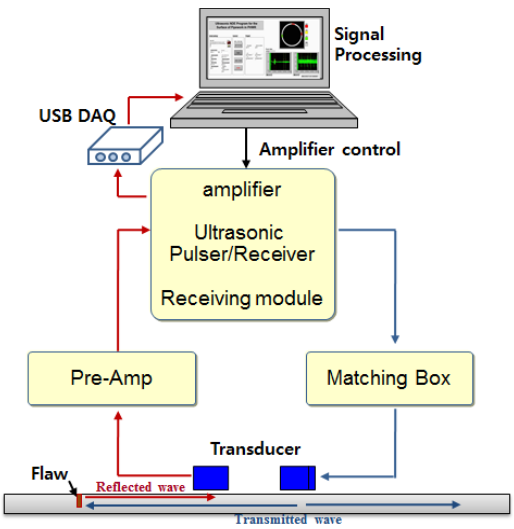

Fig.15 Schematic diagram of the EMAT experimental system

Fig.16 Picture of the SH-EMAT experimental system

To operate the EMATs, an ultrasonic inspection system consists of a pulser/receiver (Ritec, RAM 10000) for generating and receiving ultrasonic waves, an impedance matching system, a pre-amplifier for amplifying received signals (WIS, EMAT pre-Amplifier), a digitizer (NI, USB-5133) for data acquisition and the signal process software. An ultrasonic testing device usually includes a scope for evaluating signals. In this research a signal processing program is developed and applied to the pipe inspection system instead of the scope for a data acquisition and analyzing of the SH-wave signal effectively. The program is implemented by coding a program using LabVIEW software. Fig. 14 shows the developed signal processing software. The control panels are placed in the left half side of the monitor and the visualization of the signal is displayed in the right hand side. Also, Fig. 15 shows the schematic diagram of the EMAT experimental system and Fig. 16 is a picture of the SH-EMAT experimental system.

3.2.2 Pipe inspection using EMAT

In general, SH-waves have various modes and dispersion characteristics. The modes could be changed in the group velocities by their frequencies and the thicknesses of specimens. Particularly, defects in structures induce changes of the thickness, and that leads to changes in the velocities of modes. Changes of the velocities can bring out a superposition of the modes in time region. SH_0 mode which is one of the SH-wave modes has no changes in velocities according to variation in thicknesses. So, if SH_0 mode is applied, the defects are possible to detect and analyze. A proper frequency could generate a SH_0 mode by the relationship between the wavelength and the phase velocity. The proper frequency could be selected in a dispersion diagram to generate specific mode. Theoretically, the detectable minimum size of a defect by ultrasonic waves is proportional to the wavelength of the ultrasonic waves. So, the usage of a shorter wavelength can lead to more precise detection of defect. However, it easily causes mode-superposition because of the closeness of two frequencies that generate the SH_0 mode and the SH_1mode individually.

In this study, SH-EMATs with a wavelength of 5.2 mm are applied to detect the minimum size defect (3 mm x 2 mm) in the pipe specimen and consider the superposition in modes. In order to generate the SH_0 mode, the pulser is operated with a frequency of 597 kHz. Fig. 17 indicates the amplitudes of received ultrasonic waves which propagate from specimens with different notch size defects, according to flying time. The signals include signals directly transmitted from the transmitting EMAT to the receiving EMAT and signals reflected from the defect zone to the receiving EMAT. From the analysis of the SH_0 signals, it is verified that signals reflected from the defect of which size is more than 15 mm^2 (5 mm × 3 mm) can be easily identified due to their high amplitudes. However, it is hard to recognize defects with areas under 6 mm^2 (3 mm × 2 mm), due to low signal to noise ratio. Particularly, the amplitudes of the ultrasonic waves directly transmitted from the transmitting EMAT to the receiving EMAT in each test signal, show differences in each other, as shown in the dashed line box of Fig. 17. Originally, by experimental conditions such as lift-off and the contact condition of the EMAT, the intensities of the initiated ultrasonic waves are different from each other. Furthermore, the SH-waves generated by the EMAT would include other modes by superposition, even if the pulser could be controlled precisely. Thus, it is not possible to define defects simply using only the amplitudes of reflected signals.

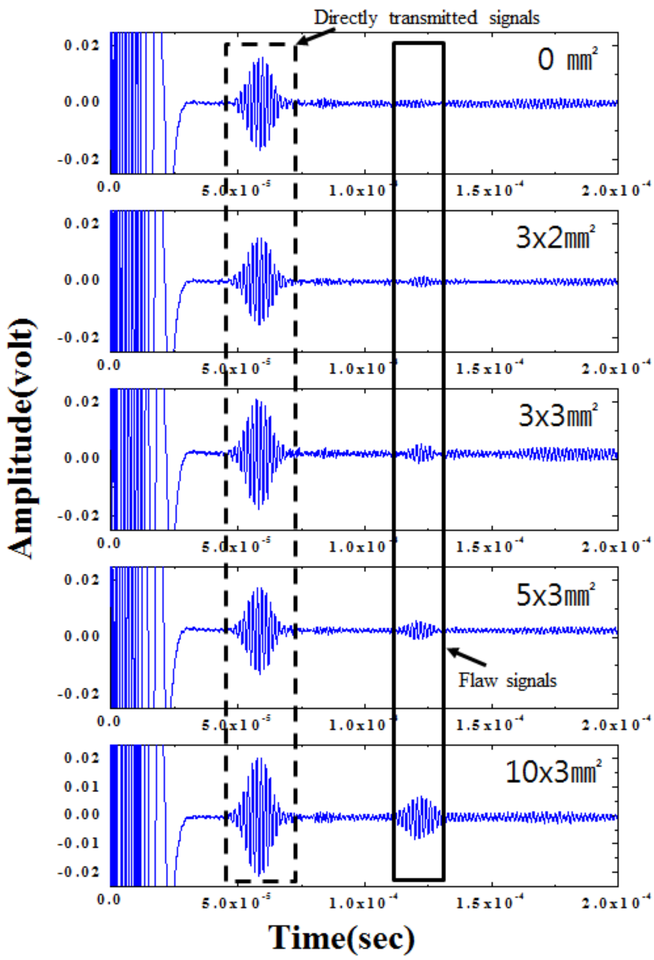

Fig.17 SH-waves time histories in the pipe for each notch zone

3.3 Signal processing based on wavelet transform

SH-EAMT signals can be propagated in different modes with various group velocities according to the frequencies and thickness of a specimen. Therefore, it is necessary to analyze the desired signals in a specific mode, using a frequency analysis according to the times of the signals in the evaluation of defects using SH-EMAT. Wavelet transforms are a good technique of changing the scale of transform time regions according to variations in frequencies. That is, the SH-EMAT signals can be analyzed by frequency analysis according to times by using such wavelet transforms, and that makes it possible to extract and analyze signals in the desired mode, which has specific frequencies (Varma *et al.* 2004).

A continuous wavelet transform (CWT) is defined as a transform function, $F(a, b)$, in which a signal, f(t), can be analyzed using a wavelet function, $\psi_{a,b}$, as shown in Eq. (1). Here, $\psi^*$is a complex conjugate function of ψ. $\psi_{a,b}$ is a mother wavelet that transforms signals to a time-frequency function according to the scale parameter, aa, and position parameter, b. The mother wavelet can be defined as Eq. (2) For processing complex function type signals, the Morlet wavelet, which is a Gaussian function, has been largely used as the mother wavelet. The Morlet wavelet is defined as Eq. (3) and should satisfy the allowance condition, $\omega_0 \geq 2\pi\beta$, because this function is to represent values in a specific region without any divergences (Varma *et al.* 2004, Mertins 1999, Park and Ahn 2001, Büssow2007, Lee and Kim 2012).

$$F(a, b) = \int_{-\infty}^{\infty} f(t)\psi^*{}_{a,b}(t)\, dt \tag{1}$$

$$\psi_{a,b}(t) = \frac{1}{\sqrt{|a|}}\psi\left(\frac{t-b}{a}\right), \quad a > 0 \tag{2}$$

$$\psi(t) = e^{i\omega_0 t}e^{-\beta t^2/2} \tag{3}$$

To use the wavelet transform in analyzing waveforms that exhibit a characteristic of dispersion like shear horizontal waves, the relationship between the dispersiveness and the wavelet constant is considered. Parameters that represent the highest wavelet amplitude in a dispersive wave, which has the center frequency of ω, group velocity of c_g, and movement of x, can be calculated using Eq. (4).

$$a = \frac{\omega_0}{\omega}, \quad b = \frac{x}{c_g} \tag{4}$$

That is, as the signal, $f(t)$, has a frequency component corresponding to the scale parameter of a, it makes it possible to analyze its frequency components, because the frequency components of the signal represent large amplitude values from the wavelet transform in the position region of b where the frequency components are presented (Mertins 1999, Park and Ahn 2001, Büssow2007, Lee and Kim 2012). In this paper, the wavelet transform is carried out by coding a program using MATLAB software. In this program, a looping statement is used in order to analyze the frequency range from 10 kHz to1.2 MHz. Here, the basic form of the ultrasonic signal is a sinusoidal, so $\omega_0 = 2\pi$ was applied.

Also, the looping statement is applied to calculate the position parameter of ‘b’ in Eq. (4); the movement ‘x’ is increased from a sample time to a total time length of 2.0×10^{-4}sec. In addition, an ultrasonic test is a comparative test basically. So, reflected signals should be evaluated with a specific sensitivity to determine as a defect. That means that it is necessary to confirm the intensity of the reflected signal according to the intensity of transmitted ultrasonic waves to verify the intensity of signals reflected from defects. Particularly, the intensity of the directly transmitted signals from the transmitting EMAT to the receiving EMAT is used as the reference intensity. Here, the wavelet transform of signals is implemented in SH-waves signals for evaluating defects using a SH_0 mode. The maximum intensity of the directly transmitted signals in the wavelet transformed spectrum is used to determine the specific sensitivity, as shown in Fig. 18, instead of using a specific sensitivity in a reference block.

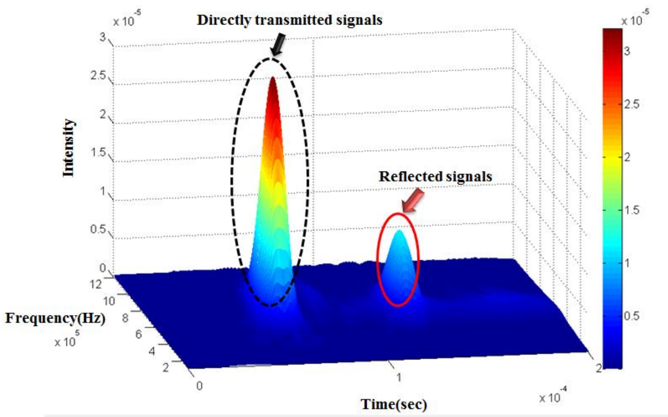

Fig. 18 Spectrum of wavelet transformed SH-wave signals from the pipe specimen with 10x3 mm^2 notch flaw

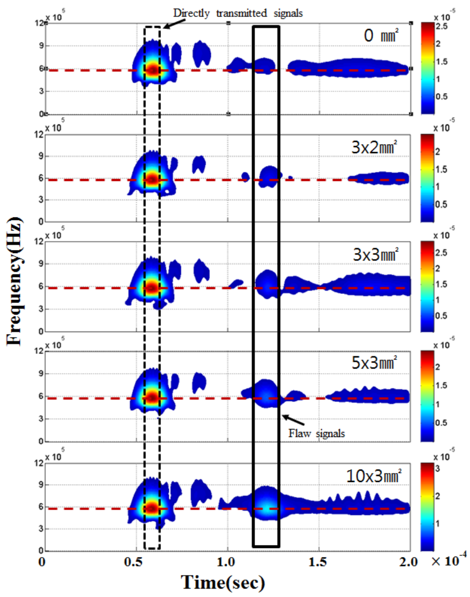

Fig. 19 SH-wave intensity according to frequency and time histories in the pipe at each notch zone

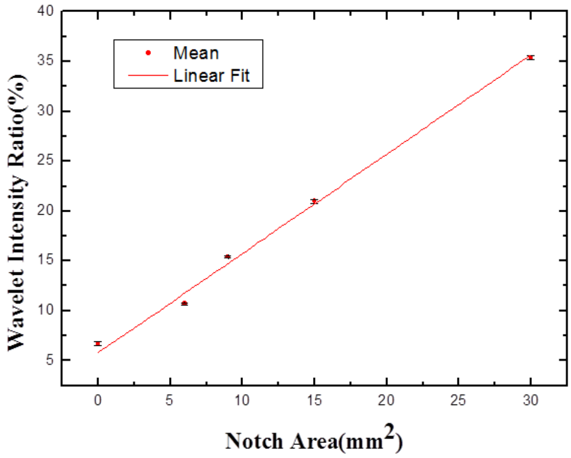

Fig. 20 Intensities ratio between the defect area signal and the directed transmitted waves signal

Fig. 19 shows the spectrum result after applying the wavelet transforms of the transferred SH waves in the defect specimen. The ratio of the intensities between the directly transferred wave signals and the reflected wave signals is used to evaluate of the defect area with the intensity of the signal component of 597 kHz. Fig. 20 shows mean values of the intensity ratio which are averaged with 10 times repeated experiment results and standard deviation (95% confidence interval). As a result, the intensity ratio increases almost linearly with increase in the defect area. That is, the wavelet transforms can be very profitable for extracting meaningful information from signals. In addition, pipe testing using SH-EMATs are quantitatively evaluated by an analysis of the signal intensity ratio.

4. Pipe Inspection by robotic system with EMATs

4.1 Pipe Inspection setup

In a main experiment, the developed robot system with EMATs was applied to pipe inspection tests. To verify a mobility performance of the robot and evaluate integrity of the pipe, a test-bed was constructed with several pipes. One of the pipes in test-bed is the defect specimen which is used for the pipe inspection using EMATs as mentioned in section 3.3. Fig. 21 shows a configuration of the inspection robot system with EMATs. The robot system moves on the pipe according to longitudinal direction. To inspect the pipe, the robot fixed at the longitudinal direction. Then the robot rotates to the circumferential direction on the pipe. As the same time, EMATs perform the pipe inspection by the generating and receiving SH-waves. Also, the ultrasonic inspection system using EMATs is constructed as same as described in Section 3.3. Fig. 22 shows the pipe test-bed, the inspection robot and the EMAT ultrasonic system. Fig. 23 shows the robot system with EMATs in detail. In the test, the receiver EMAT acquired signals with 115 mm distance from the defects.

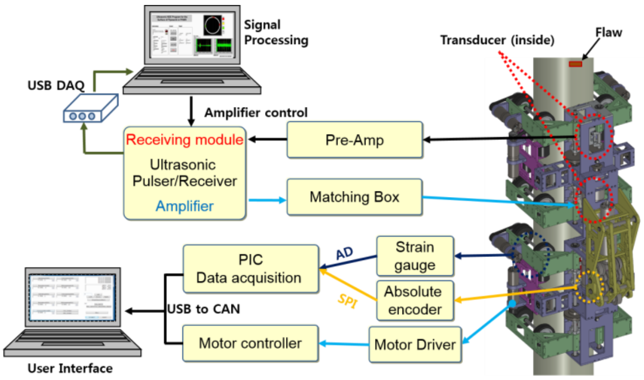

Fig. 21 schematic diagram of an inspection robot system with EMATs

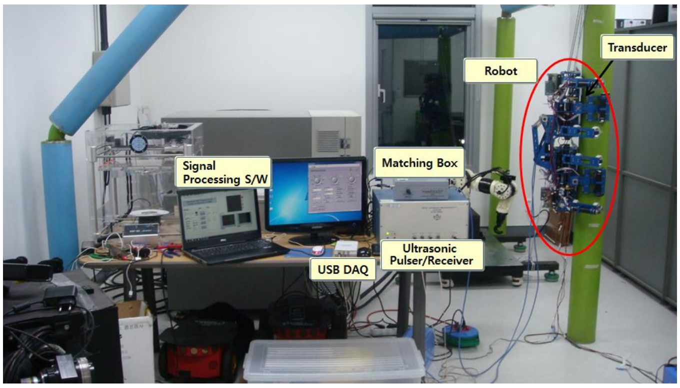

Fig. 22 Picture of pipe inspection using robot system

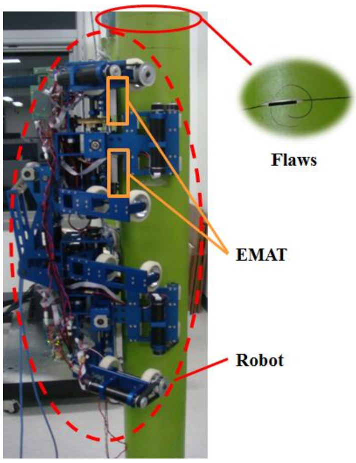

Fig. 23 Picture of pipe inspection using robot system

4.2 Pipe inspection result

As shown in Fig. 24 that indicates an inspection result with the robot system, directly transmitted signals and reflected signals were successfully acquired. The reflected signals from the defects were collected with an exact distance (115 mm) from receiver EMAT to the defect, in the time region. From the results of the amplitude signals received from the SH_0, it was verified that defect signals from defect areas more than 15 mm^2 (5 mm × 3 mm) can be easily identified too. However, it is hard to identify their dispersion and superposition of the modes in cases of defect signals under 6 mm^2 (3 mm × 2 mm) area. So, the signal processing based on wavelet transforms, as described in section 3.4, was applied to evaluate the signals. Fig. 25 shows the spectrum result after applying the wavelet transforms.

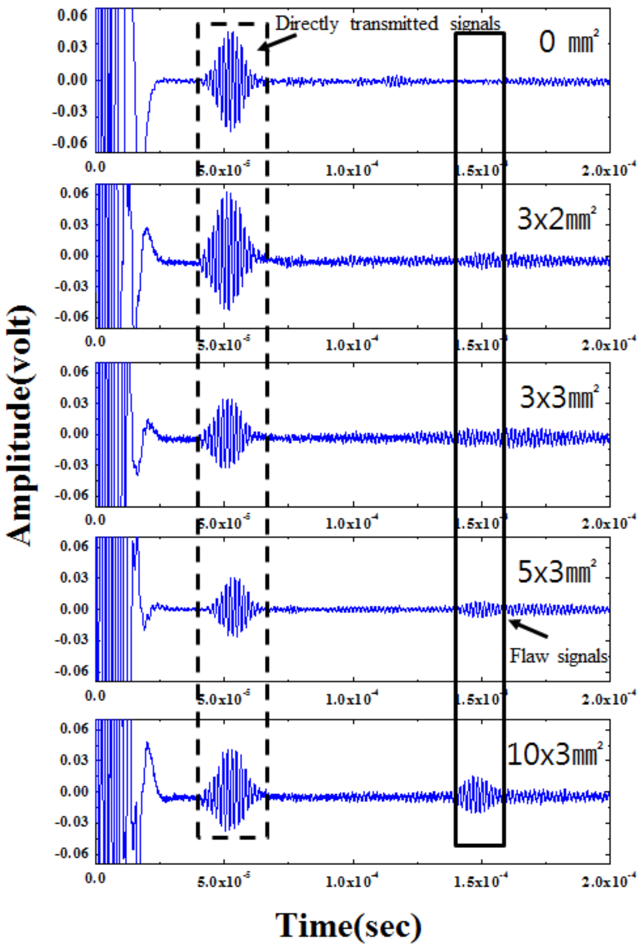

Fig. 24 SH-waves time histories in the pipe for each notch zone acquired by inspection robot

Based on the intensity of the signal component of 597 kHz, evaluation of the defect area was performed using the intensity ratio too, as shown in Fig. 26. As a result, it was verified that the intensity ratio increased linearly with increases in the defect area like in section 3.4. Even if the ratio of the 6 mm^2 area defect shows some errors with the fitted line, it could be evaluated qualitatively.

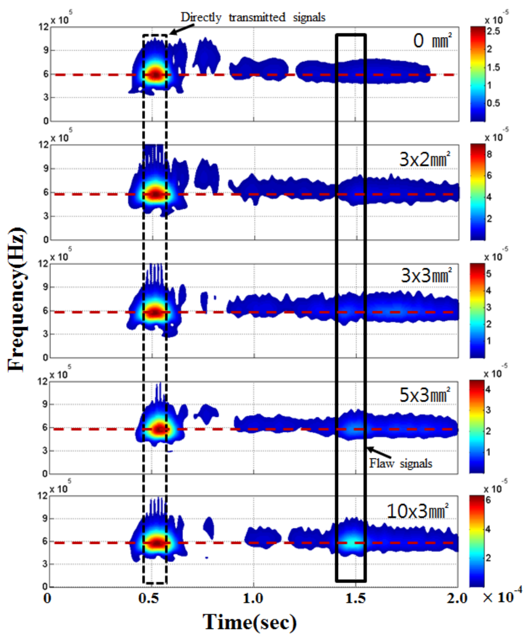

Fig. 25 SH-wave intensity according to frequency and time histories in the pipe at each notch zone

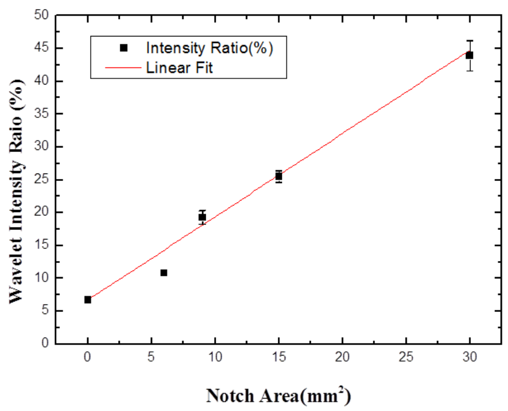

Fig. 26 Relationship between the defect area and the ratio of the maximum intensities of two key spectrum results

5. Conclusions

In this study, to evaluate the integrity of pipe structures, a robotic ultrasonic inspection system is proposed. The robotic system is developed to overcome an obstacle with high mobility. For inspection of pipe structure, SH-waves generated by EMAT is applied with additional signal processing methods. Two-module mobile robot platform could move over the T-branch pipe joint and move along the straight pipeline at 12 cm/s. The SH_0 mode, which has no changes in velocities, is applied to evaluate the position and size of defects in a pipe using SH-EMAT.A wavelet transform is implemented to extract a meaningful and specific signal from the superposed SH-wave signals. Intensity ratio which is normalized the defect signals intensity by the maximum intensity of directly transmitted signals in the wavelet transforms spectrum is applied to evaluate defects quantitatively. Finally, it is verified that the robotic ultrasonic inspection system with EMAT can implement of inspection and evaluate defects in pipe structure successfully by applying signal processing method based on wavelet transform.

Acknowledgements

This work was supported in part by the Human Resources Development program (No.20101620100110) of the Korea Institute of Energy Technology Evaluation and Planning(KETEP) grant funded by the Korea government Ministry of Trade, Industry and Energy, and also in part by Basic Science Research Program through the National Research Foundation of Korea (NRF) funded by the Ministry of Education, Science and Technology (NRF-2013R1A1A2013636).

References

Büssow, R. (2007), "An Algorithm for the continuous Morlet wavelet transform", *Mech. Syst. Signal Pr.*, **21**(8), 2970-2979.

Fujisawa, K. (2002), "Application of EMAT to steel and nonferrous metal", *J. JSNDI*, **51**(2), 68-73.

Fukuda, T., Hosokai, H. and Otsuka, M (1987), "Autonomous pipeline inspection and maintenance robot with inch worm mobile mechanism", *Proceedings of the IEEE International Conference on Robotics and Automation*.

Gori, M., Giamboni, S., D'Alessio, E., Ghia, S., Cernuschi, F. and Piana, G.M. (1996), "Guided waves by EMAT transducers for rapid defect location onheat exchanger and boiler tubes", *Ultrasonics*, **34**, 311-314.

Hirao, M. and Ogi, H. (1999),"An SH-wave EMAT technique for gas pipeline inspection", *NDT&E Int.*, **32**(3), 127-132.

Hirao, M. and Ogi, H. (2003), *EMATs for science and industry: noncontacting ultrasonic measurements*, Kluwer Academic Publisher, Boston, USA.

Kawasaki, H. and Murakami, S. (2008), "Novel climbing method of pruning robot", *Proceedings of the SICE Annual Conference*, Tokyo, Japan, Aug.

Kim, S. and Choi, S. (2005), "The robotic technology applications on nuclear power plants in Korea", *J. Robot. Soc. Japan*, **23(**5), 548-551.

Kim, S., Spenko, M., Trujillo, S., Heyneman, B., Mattoli, V. and Cutkosky, M.R. (2007), "Whole body adhesion: hierarchical, directional and distributed control of adhesive forces for a climbing robot", *Proceedings of the IEEE International Conference on Robotics and Automation*, Roma, Italy, Apr.

Lee, J.H., Park, L.K., Kim, Y.K and Kim, D.H (2011), "Evaluation of thickness reduction in steel plate by using SH-EMATs", *J. KSNT*, **31**(1), 38-43.

Lee, J.H. and Kim, D.H. (2012), "Flaw-detection of pipes-welded zone by using wavelet transform and SH-EMAT", *T. KSME*, **36**(12) 1511-1519.

Lei, K., Wujun, M., Chao, L. and Shujuan, W. (2008), "Research on weak signal detection technique for electromagnetic ultrasonic inspection system", *Proceedings of the IEEE Conference of Industrial Electronics and Applications*,Singapore, June.

Lipkin, K., Borwn, I., Peck, A., Choset, H., Rembisz, J., Gainfortoni, P. and Naaktgeboren, A. (2007), "Differentiable and piecewise differentiable gaits for snake robots", *Proceedings of the IEEE/RSJ International Conference on Intelligent Robots and Systems*, San Diego, USA, Oct.

Liu, S., Dua, C., Moua, J., Martua, L., Zhang, J. and Lewis, F.L. (2013), "Diagnosis of structural crack susing wavelet transform and neural", *NDT&E Int.*, **54**, 9-18.

Mertins, A. (1999), *Signal analysis: wavelets, filter banks, time-frequency transforms, and applications*, WILEY, Chichester, England.

Noohi, E., Mahdavi, S.S., Baghani, A. and Ahmadabadi, M.N. (2010), "Wheel-based climbing robot: modeling and control", *Adv. Robotics*, **24(**8-9), 1313-1343.

Park, I.K. and Ahn, H.K. (2001), "Time-frequency analysis of lamb wave mode", *J. KSMTE*, **10**(1), 133-140.

Park, I.K., Kim, H.M., Park, T.S., Kim, Y.G., Cho, Y.S. and Song, W.J. (2006), "Non-contact ultrasonic inspection technology of fillet weldments monitoring", *Key Eng. Mater.*, **321-323**, 513-517.

Parker, L.E. and Draper, J.V. (1998), *Handbook of industrial robotics*, (2nd Ed.), John Wiley, New York, NY, USA.

Roh, S. and Choi, H.R. (2005), "Differential-drive in-pipe robot for moving inside urban gas pipelines", *IEEE T. Robot*., **21**(1), 1-17.

Roh, S., Kim, D.W., Lee, J.S., Moon, H. and Choi, H.R. (2009), "In-pipe robot based on selective drive mechanism", *Int. J. Control Autom*., **7**(1), 105-112.

Soto-Cajiga, J.A., Pedraza-Ortega, J.C., Rubio-Gonzalez, C., Bandala-Sanchez, M., Romero-Troncoso, R. de J. (2012), "FPGA-based architecture for real-time data reduction of ultrasound signals", *Ultrasonics*, **52**(2), 230-237.

Tavakoli, M., Marques, L. and Almeida, A.T. (2011), "3DCLIMBER: climbing and manipulation over 3D structures", *Mechatronics*, **21**(1), 48-62.

Varma, V.K., Tucker R., Kercel, S., Rose, J., Luo, W. and Zhao, X. (2004), "Pipeline flaw detection using shear EMAT and wavelet analysis", *GTI's Natural Gas Technologies II*, Pheonix, AZ, USA.

Xu, F. and Wang, X. (2008), "A wheel-based cable climbing robot with descending speed restriction", *Proceedings of the Chinese control and Decision Conference*, Shangdong, China, July.